Ab initio Study on Structures, Energies and Vibrations of Methylammonium-(water)ₙ (*n*=1-3) Complexes

Kwang-Yon Kim, Ung-In Cho, and Doo Wan Boo*

Department of Chemistry, Yonsei University, Seoul 120-749, Korea
Received April 12, 2001

The B3LYP/6-31+G(d) calculations on the structures, the hydration energies, the thermodynamic functions, and the vibrations of various isomers of $CH_3NH_3^+(H_2O)_n$ (*n*=1, 2, 3) have been performed. Results indicate that not only the direct charge-dipole two-body interactions, but also the three-body interactions involving water-water hydrogen bonding and indirect charge-dipole interactions play significant roles in determining the overall structures and relative stabilities of isomers. Particularly, the hydrogen bond cooperativity plays a critical role in stabilizing the cyclic isomer *vs*. tripod isomer for *n*=3. The calculated thermodynamic functions match well the recent experimental thermodynamic functions by Meot-Ner within 1 kcal/mol. The trends of calculated hydration energies and vibrational frequencies correlate excellently with the local many-body hydrogen bond interactions in each isomer. Finally, it is proposed that the distinct spectral patterns of bonded-NH, bonded-OH, and free OH stretches can be used as fingerprints in identifying the structural isomers that contribute to the vibrational predissociation spectra.

Keywords : *Ab initio*, Solvation, Hydrogen bond cooperativity. Many-body interaction.

Introduction

The solvation structure and dynamics of ions in water play an important role in many chemical and biological processes.[1,2] The ion hydration processes in the first few solvation shells are of particular significance in determining the conformations and activities of biomolecules in water.[3,4] The hydrogen bonding networks close to the ionic chromophores are generally governed by the competition between the ion-water and water-water interactions, different from those in the bulk where the water-water interactions are dominant. During the past few decades extensive experimental and theoretical investigations[5-8] of ion-water complexes in the gas phase have been performed to better understand the nature of ion hydration. With recent advances in the accuracy and speed of quantum computations and owing to the experimental difficulties in spectroscopic measurements,[9] the *ab initio* theoretical approach has become an important tool in furnishing the detailed picture of the structures and dynamics of protonated ion-water complexes. Furthermore, the calculations serve as a useful guide for carrying out important spectroscopic measurements.

In order to describe accurately the potential energy surfaces of hydrogen bond networks of protonated biomolecules in the first few solvation shells where the continuum model[10,11] fails to predict, we have initiated the systematic *ab initio* quantum mechanical and spectroscopic studies on the hydration behaviors of various types of protonated ions as a function of the number of water molecules which model the hydration of important bio-functional groups of protonated biomolecules. Previously, we have reported extensive

ab initio theoretical and vibrational predissociation spectroscopic studies of protonated ethylenediamine-(water)₃ complexes where the origins of intramolecular hydrogen bond-assisted cyclic structure formation were discussed.[12] As a continuation of the study, in this work, we investigate the hydrated structures, the hydration energies, the thermodynamic functions, and the vibrational spectra of methyl-ammonium-(water)ₙ (*n*=1, 2, 3) complexes which serve as a simplest model for understanding the hydration behaviors of the N-terminal groups of amino acids, peptides and proteins in the first and second hydration shells.

To our knowledge, no prior *ab initio* theoretical and spectroscopic studies on $CH_3NH_3^+(H_2O)_n$ have been reported although the thermodynamic functions ($\Delta H_{n-1,n}$, $\Delta G_{n-1,n}$) for the clustering reaction $CH_3NH_3^+(H_2O)_{n-1} + H_2O \rightarrow CH_3NH_3^+(H_2O)_n$ have been measured using a high-pressure mass spectrometric technique by Meot-Ner[13] and Kebarle *et al*.[14] The two sets of experimental thermodynamic functions are closely compared in this paper with our *ab initio* results. This work is an extension of previous *ab initio*[15] and vibrational predissociation spectroscopic[16] works on $NH_4^+(H_2O)_n$ by Lee *et al*., and provides a guide for carrying out vibrational predissociation measurements and also a theoretical reference for comparison with the spectroscopic results.

Computational Details

Ab initio calculations on the structural isomers, the electronic energies, and the vibrational frequencies for methyl-ammonium-(water)ₙ (*n*=1-3) complexes were performed at B3LYP/6-31+G(d) level using the Gaussian 98 package.[17] Throughout the calculations the tight convergence thresholds for both SCF energies and geometry optimizations and symmetry-unconstrained options have been employed to

ensure finding low lying structural isomers in the multidimensional potential energy surfaces. The calculated electronic energies and hydration energies for $CH_3NH_3^-(H_2O)_n$ (n=1, 2, 3) (denoted as MaW_n) are corrected by the zeropoint energies (ZPE) and basis set superposition errors (BSSE) following the procedures of Boys-Bernardi as below.[18]

$$E(\text{BSSE}) = \{E(\text{Ma}|1...n+1) - E(\text{Ma})\}$$
$$+ \sum_{i=1}^{n} \{E(W_i|1...n+1) - E(W_i)\} \qquad (1)$$

where $E(\text{Ma}|1...n+1)$ and $E(W_i|1...n+1)$ represent the electronic energies of $CH_3NH_3^+$ (or Ma) and i-th H_2O molecule (or $H_2O(i)$) with relaxed geometries in the clusters using the extended basis set for MaW_n. (*i.e.* a (n+1)-body system). The $E(\text{Ma})$ and $E(W_i)$ represent the electronic energies calculated using the same geometries but with the basis functions centered on themselves.

The total hydration energies (ΔE_n), hydration enthalpies (ΔH_n), and hydration Gibbs free energies (ΔG_n) for the clustering reaction Ma + nW → MaW_n at two temperatures (298 K, 150 K) were calculated according to the following equations:

$$\Delta E_n = E_{MaW_n} - (E_{Ma} + nE_W)$$
$$\Delta H_n = H_{MaW_n} - (H_{Ma} + nH_W)$$
$$\Delta G_n = G_{MaW_n} - (G_{Ma} + nG_W) \qquad (2)$$

The stepwise hydration energies ($\Delta E_{n-1,n}$), hydration enthalpies ($\Delta H_{n-1,n}$), and Gibbs free energies ($\Delta G_{n-1,n}$) for the reaction MaW_{n-1} + W → MaW_n were calculated as followings:

$$\Delta E_{n-1,n} = E_{MaW_n} - (E_{MaW_{n-1}} + E_W)$$
$$\Delta H_{n-1,n} = H_{MaW_n} - (H_{MaW_{n-1}} + H_W)$$
$$\Delta G_{n-1,n} = G_{MaW_n} - (G_{MaW_{n-1}} + G_W) \qquad (3)$$

In order to take into account the effects of electron correlations and anharmonicities, the calculated harmonic frequencies were multiplied by 0.973, an empirical scaling factor previously determined from the correlation between the calculated frequencies at B3LYP/6-31+G(d) level and the observed frequencies.[16] All the calculations in this work were performed in the Digital-Alpha workstation and SGI Origin2000.

Results and Discussion

Geometries and Energetics. The representative low-lying structural isomers for methylammonium-(water)$_n$ (n=1-3) complexes optimized at B3LYP/6-31+G(d) level are depicted in Figure 1, and their selected geometric parameters including those of free methylammonium (Ma) are listed in Table 1. The calculated electronic energies for individual isomers with BSSE and ZPE corrections, and the relative energetics are illustrated in Table 2. Due to the superior
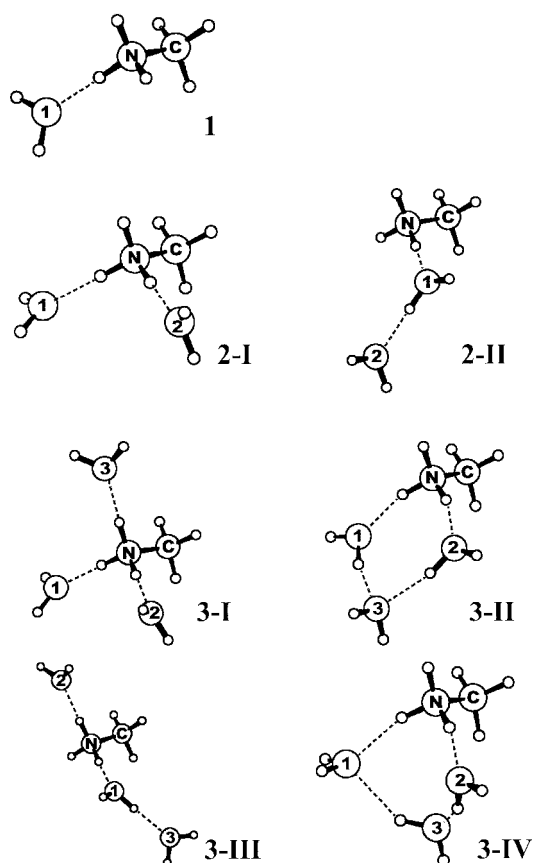
Figure 1. *Ab initio* optimized structures of $CH_3NH_3^-(H_2O)_n$ (n=1-3) at B3LYP/6-31+G(d) level. The oxygen atoms of the water molecules in each isomer are numbered for the discussion purposes.

strengths of charge-dipole interactions, the water molecules in the complexes are bonded exclusively to the -NH_3^- moiety of the Ma core consistent with the asymmetric hydration behavior of a protonated amphiphilic chromophore.[19] For n=1, isomer **1** is the lowest energy isomer with the water molecule charge-dipole bonded to a proton of -NH_3 moiety in a C_{2v} fashion. The ionic hydrogen bonding is characterized by the hydrogen bond lengths of $R(H_N^1O_1) = 1.72$ Å, $R(NO_1)$=2.78 Å, the hydrogen bond angle of $\angle NH_N^1O_1$ =178.3°, and the bonded N-H of $R(NH_N^1)$=1.05 Å slightly lengthened from that of isolated Ma (1.03 Å) (see Table 1 for the notations).

For n=2, there are two isomeric forms, one with two charge-dipole bonds (**2-I**) and the other with one charge-dipole bond and one water-water hydrogen bond (**2-II**). The two water molecules forming the first solvation shell (denoted as $1°H_2O$) in isomer **2-I** play roles as the core proton acceptors (A) while the $1°H_2O$, $2°H_2O$ (second shell) molecules in isomer **2-II** as the core proton acceptor and water proton donor (Ad), and the water proton acceptor (a), respectively. The strengths of individual charge-dipole bonds of isomer **2-I** are somewhat weakened compared to isomer **1** due to the reduced charge density of each bonded proton resulting in the increased hydrogen bond lengths

Table 1. Optimized geometric parameters for structural isomers of $CH_3NH_3^+(H_2O)_n$ (n=0-3). Distances (R) are in angstroms, and bending angles ($\angle$), dihedral angles (D) are in degrees

Structures	Geometric Parameters[a]
Ma	$R(NH_N)$=1.03, $R(CH_C)$=1.09, $R(NC)$=1.52, $\angle(CNH_N)$=111.6, $\angle(NCH_C)$=108.2, $\angle(H_NNH_N)$=107.3, $\angle(H_CCH_C)$=110.7
1	$R(NH_N^1)$=1.05, $R(NH_N)$=1.03, $R(NO_1)$=2.78, $R(O_1H_1)$=0.97, $R(H_N^1 O_1)$=1.72, $\angle CNH_N^1$=111.5, $\angle(CNH_N)$=111.3, $\angle(H_N^1 NH_N)$=107.7, $H_N^1 (H_NNH_N)$=106.9, $\angle(CNO_1)$=110.4, $\angle(NH_N^1 O_1)$=178.3, $D(O_1NCH_N^1)$=0.1
2-I	$R(NH_N^1)$=$R(NH_N^2)$=1.04, $R(NH_N)$=1.02, $R(NO_1)$=$R(NO_2)$=2.82, $R(H_N^1 O_1)$=$R(H_N^2 O_2)$=1.78, $R(O_1O_2)$=4.64, $\angle(H_N^1 NH_N)$=107.4, $\angle(H_N^2 NH_N)$=107.5, $\angle(H_N^1 NH_N^2)$=108.4, $\angle(O_1NH)$=110.3, $\angle(O_2NC)$=109.3, $\angle(O_1NO_2)$=110.6, $\angle(NH_N^1 O_1)$=178.4, $\angle(NH_N^2 O_2)$=177.0, $D(O_1NCH_N^1)$=0.0, $D(O_2NCH_N^2)$=1.0, $D(O_1NCO_2)$=-121.8
2-II	$R(NH_N^1)$=1.06, $R(NH_N)$=1.03, $R(NO_1)$=2.69, $R(NO_2)$=4.67, $R(O_1O_2)$=2.72, $R(H_N^1 O_1)$=1.63, $R(H_1^2 O_2)$=1.74, $\angle(H_N^1 NH_N)$=107.7, $\angle(H_NNH_N)$=107.0, $\angle(O_1NC)$=110.7, $\angle(O_2NC)$=124.6, $\angle(NO_1O_2)$=119.1, $\angle(NH_N^1 O_1)$=177.1, $\angle(O_1H_1^2 O_2)$=173.7, $D(O_1NCH_N^1)$=-1.7, $D(O_1NCO_2)$=31.1, $D(O_2O_1NC)$=-123.6
3-I	$R(NH_N^1)$=$R(NH_N^2)$=$R(NH_N^3)$=1.04, $R(NO_1)$=$R(NO_2)$=$R(NO_3)$=2.86, $R(O_1O_2)$=4.69, $R(O_1O_3)$=4.68, $R(O_2O_3)$=4.69, $R(H_N^1 O_1)$=1.82, $R(H_N^2 O_2)$=1.82, $R(H_N^3 O_3)$=1.83, $\angle(H_N^1 NH_N^2)$= $\angle(H_N^2 NH_N^3)$= $\angle(H_N^3 NH_N^1)$=108.1, $\angle(O_1NC)$=109.0, $\angle(O_2NC)$=109.2, $\angle(O_3NC)$=108.9, $\angle(O_1NO_2)$=110.0, $\angle(O_1NO_3)$=110.1, $\angle(O_2NO_3)$=109.6, $\angle(NH_N^1 O_1)$=177.0, $\angle(NH_N^2 O_2)$=177.2, $\angle(NH_N^3 O_3)$=177.0, $D(O_1NCH_N^1)$=0.6, $D(O_2NCH_N^2)$=0.8, $D(O_3NCH_N^3)$=0.6
3-II	$R(NH_N^1)$=$R(NH_N^2)$=1.05, $R(NH_N)$=1.02, $R(NO_1)$=$R(NO_2)$=2.77, $R(NO_3)$=4.30, $R(O_1O_2)$=3.65, $R(O_1O_3)$=$R(O_2O_3)$=2.87, $R(H_N^1 O_1)$=$R(H_N^2 O_2)$=1.76, $R(H_1^3 O_3)$=1.93, $R(H_2^3 O_3)$=1.92, $\angle(H_N^1 NH_N)$= $\angle(H_N^2 NH_N)$=108.3, $\angle(H_N^1 NH_N^2)$=104.4, $\angle(O_1NC)$=115.4, $\angle(O_2NC)$=115.5, $\angle(O_3NC)$=126.0, $\angle(O_1NO_2)$=82.4, $\angle(O_1O_3O_2)$=79.0, $\angle(NO_1O_3)$= $\angle(NO_2O_3)$=99.3, $\angle(NH_N^1 O_1)$= $\angle(NH_N^2 O_2)$=162.2, $\angle(O_1H_1^3 O_3)$= $\angle(O_2H_2^3 O_3)$=160.7, $D(O_1NCH_N^1)$=11.5, $D(O_2NCH_N^2)$=-11.5, $D(O_1NCO_2)$=-93.7, $D(O_2O_2O_1N)$=177.9
3-III	$R(NH_N^1)$=1.05, $R(NH_N^2)$=1.04, $R(NH_N)$=1.02, $R(NO_1)$=2.74, $R(NO_2)$=2.84, $R(NO_3)$=4.76, $R(O_1O_2)$=4.63, $R(O_1O_3)$=2.75, $R(H_N^1 O_1)$=1.69, $R(H_N^2 O_2)$=1.80, $R(H_1^3 O_3)$=1.76, $\angle(H_N^1 NH_N)$=107.4, $\angle(H_N^2 NH_N)$=107.6, $\angle(H_N^1 NH_N^2)$=108.7, $\angle(O_1NC)$=108.4, $\angle(O_2NC)$=109.1, $\angle(O_3NC)$=82.4, $\angle(O_1NO_2)$=111.9, $\angle(NO_1O_3)$=120.3, $\angle(NH_N^1 O_1)$=175.9, $\angle(NH_N^2 O_2)$=176.8, $\angle(O_1H_1^3 O_3)$=174.4, $D(O_1NCH_N^1)$=-0.6, $D(O_2NCH_N^2)$=0.5, $D(O_1NCO_2)$=-122.1, $D(O_1NCO_3)$=14.8, $D(O_3O_1NC)$=-30.5
3-IV	$R(NH_N^1)$=1.04, $R(NH_N^2)$=1.06, $R(NH_N)$=1.02, $R(NO_1)$=2.96, $R(NO_2)$=2.71, $R(NO_3)$=3.37, $R(O_1O_2)$=3.85, $R(O_1O_3)$=2.90, $R(O_2O_3)$=2.73, $R(H_N^1 O_1)$=1.95, $R(H_N^2 O_2)$=1.69, $R(H_2^3 O_3)$=1.86, $R(H_1^3 O_1)$=2.06, $\angle(H_N^1 NH_N)$=108.3, $\angle(H_N^2 NH_N)$=108.7, $\angle(H_N^1 NH_N^2)$=105.5, $\angle(O_1NC)$=112.4, $\angle(O_2NC)$=111.7, $\angle(O_3NC)$=85.6, $\angle(O_1NO_2)$=85.5, $\angle(NO_1O_3)$=70.1, $\angle(NO_2O_3)$=76.5, $\angle(O_1O_3O_2)$=86.2, $\angle(NH_N^1 O_1)$=164.0, $\angle(NH_N^2 O_2)$=161.9, $\angle(O_2H_2^3 O_3)$=145.3, $\angle(O_3H_1^3 O_1)$=143.2, $D(O_1NCH_N^1)$=11.2, $D(O_2NCH_N^3)$=-12.0, $D(O_1NCO_2)$=-94.1, $D(O_2NCO_3)$=45.9, $D(O_3O_2O_1N)$=-109.3

[a]H_j^i denotes the hydrogen atom covalent-bonded to j atom (j=N, C) and hydrogen-bonded to $H_2O(i)$ (i=1, 2, 3) according to Figure 1. O_i denotes the oxygen atom in $H_2O(i)$.

Table 2. Electronic energies (E_{el}) of structural isomers of $CH_3NH_3^+(H_2O)_n$ (n=0-3) at B3LYP/6-31+G(d). All the absolute energies are in hartree, and the relative energies in parentheses are in kcal/mol

	E_{el}	E_{el} + BSSE	E_{el} + BSSE + ZPE
Ma	-96.216015		-96.136222[a]
1	-172.670024	-172.668154	-172.564567
2-I	-249.119390 (0)	-249.115714 (0)	-248.988401 (0)
2-II	-249.116680 (1.70)	-249.112608 (1.95)	-248.984464 (2.47)
3-I	-325.565126 (1.53)	-325.559625 (0.82)	-325.408880 (0)
3-II	-325.567568 (0)	-325.560934 (0)	-325.407098 (1.12)
3-III	-325.564058 (2.20)	-325.558263 (1.68)	-325.406474 (1.51)
3-IV	-325.561873 (3.57)	-325.555557 (3.37)	-325.401463 (4.65)

[a]Only ZPE-corrected.

($R(H_N^1 O_1)$=1.72 Å, $R(NO_1)$=2.78 Å) with almost linear hydrogen bond angles ($\angle NH_N^1 O_1$ =178.4°, $\angle NH_N^2 O_2$ = 177.0°). Conversely, the charge-dipole bond lengths in isomer **2-II** ($R(H_N^1 O_1)$=1.63 Å, $R(NO_1)$=2.69 Å) are shorter than those of isomers **1**. **2-I** due to the localized charge density at single proton (H_N^1). The water-water hydrogen bond lengths and angles in isomer **2-II** are maintained at $R(H_1^2 O_2)$=1.74 Å, $R(O_1O_2)$=2.72 Å. $\angle O_1 H_1^2 O_2$=173.7°. Of particular interest is that the energy difference between isomers **2-I** and **2-II** with BSSE and ZPE corrections is only 2.47 kcal/mol. much smaller than the estimated value (~8 kcal/mol) only from the typical pairwise additive two-body interaction energies of proton-1°H₂O (~18 kcal/mol). proton-2°H₂O (~6 kcal/mol), and 1°H₂O-2°H₂O (~4 kcal/mol).[12] This result suggests that the stronger nonadditive three-body attractive interactions (or hydrogen bond cooperativity) for isomer **2-II** *vs.* isomer **2-I** due to the homodromic hydrogen bond network for the former play an important role in reducing the two-body energy difference between two isomers.

For n=3, there are four types of low-lying isomers. Isomer **3-I** corresponds to a tripod isomer with three charge-dipole

bonded $1°H_2O$ molecules playing as the core proton acceptors (A). Due to further reduced charge densities. the charge-dipole bonds are further lengthened from those of isomer **2-I**, and the hydrogen bond angles are maintained almost linear $(R(H_K^1 O_1)=1.82$ Å. $R(NO_1)=2.86$ Å, $\angle NH_N^1 O_1 =177°)$. In isomer **3-II**, the three water molecules form a cyclic ion-(water)$_3$ structure with two charge-dipole bonds and two water-water hydrogen bonds. The $1°H_2O(1.2)$ and $2°H_2O(3)$ molecules act as the core proton acceptor and water proton donors (Ad). and the water proton double acceptor (aa). respectively. Due to the geometrical constraints by ring closure. the charge-dipole and water-water hydrogen bond angles as well as the bonded H-N-H angles are significantly bent from those of non-cyclic isomers: $\angle NH_K^1 O_1 =162.2°$. $\angle O_1 H_1^3 O_3 =160.7°$. $\angle H_K^1 NH_N^2 =104.4°$. Isomer **3-III** is a open structure which can be formed via simple bond rupture of one of the water-water hydrogen bonds in isomer **3-II** alleviating the geometrical constraints ($\angle NH_K^1 O_1 =175.9°$. $\angle O_1 H_1^3 O_3 =174.4°$. $\angle H_K^1 NH_N^2 =108.7°)$. The three H_2O (1, 2, 3) molecules play roles as Ad-, A-, a-types of ligands. respectively. The cyclic structure of isomer **3-IV** is analogous to that of isomer **3-II**, but contains an asymmetric hydrogen bond network in it. The $1°H_2O(1)$ molecule act as a core proton acceptor and water proton acceptor (Aa) instead of Ad as in **3-II**. and the $1°H_2O(2)$, $2°H_2O(3)$ molecules play roles as the core proton acceptor and water proton donor (Ad) and the water proton acceptor and donor (ad). respectively. The switch-over in the roles of hydrogen bonding in **3-IV** from **3-II** results in substantial geometrical changes such as inhomogeneous hydrogen bond lengths $(R(H_N^1 O_1)=1.95$ Å. $R(H_K^2 O_2)=1.69$ Å: $R(NO_1)=2.96$ Å. $R(NO_2)=2.71$ Å) and inhomogeneous and strained hydrogen bond angles $(\angle NH_N^1 O_1 =164°$, $\angle NH_N^2 O_2 =161.9°$. $\angle O_2 H_2^3 O_3 =145.3°$. $\angle O_3 H_3^1 O_1 =143.2°)$.

As illustrated in Table 2, the relative stabilities are in the orders of **3-I** > **3-II** > **3-III** > **3-IV** with BSSE and ZPE corrections while **3-II** > **3-I** > **3-III** > **3-IV** for with BSSE corrections, and without BSSE and ZPE corrections. Of considerable interest is the greater electronic stability of isomer **3-II** vs. **3-I** despite one less charge-dipole bond for the former. The lower BSSE-corrected electronic energies for isomer **3-II** vs. **3-I** (by ~0.8 kcal/mol) cannot be explained solely by the differences of their pairwise additive two-body interactions that predict ~4 kcal/mol lower energies for isomer **3-I**. This result indicates that the hydrogen bond cooperativity plays an important role in stabilizing the cyclic isomer (**3-II**) similar to the cases of cyclic water clusters $(H_2O)_n$ $(n=3, 4, ..)$.[20] The greater hydrogen bond cooperativity for cyclic isomer (**3-II**) vs. tripod isomer (**3-I**) can be expected from the fact that the former contains the homodromic three-body hydrogen bond networks $(MaW_1W_3$. $MaW_2W_3)$ whereas the latter contains only the heterodromic three-body hydrogen bond networks.

The greater electronic stability of cyclic isomer vs. tripod isomer. however, was not seen in the case of ammonium-(water)$_3$ complexes where the tripod isomer (**3-I**) was predicted to be slightly lower in the BSSE-corrected electronic

energies than the cyclic isomer according to Chang *et al.*[15] The different hydration behavior of methylammonium compared to ammonium ion may originate from the reduced charge densities of protons and the slight geometrical changes in the $-NH_3^-$ moiety induced by methyl substitution. The calculated Mulliken charge densities of protons for isolated methylammonium and ammonium ions at B3LYP/6-31+G(d) are 0.501. 0.504, and their H-N-H angles of the NH_3^+ moieties are 107.3°, 109.47°. respectively. It is conceivable that the smaller proton charge densities for the former lead to the weaker charge-dipole interactions. and simultaneously the smaller H-N-H angles are favorable in forming a cyclic ion-(water)$_3$ structure with less geometrical strains evidenced by the slightly enlarged hydrogen bond angles for cyclic isomer of $Ma(H_2O)_3$ vs. $NH_4^+(H_2O)_3$ $(\angle NH_K^1 O_1 =162.2°$ vs. 162.0°; $\angle O_1 H_1^3 O_3 =160.7°$ vs. 159.8°).[15] The combined effects would contribute to the relative stability of cyclic isomer vs. tripod isomer in the case of methyl-ammonium-(water)$_3$ complex. Nonetheless. the tripod isomers are 1.1. 1.9 kcal/mol more stable than the cyclic isomers for both complexes with ZPE and BSSE corrections.

The BSSE-corrected energy of isomer **3-III** is 1.68 kcal/mol higher than that of isomer **3-II**, suggesting that the two-body energy loss (~4 kcal/mol) by breaking one water-water hydrogen bond in isomer **3-II** is somewhat compensated by the release of ring-strains in hydrogen bonding network and the absence of a repulsive three-body term (i.e. heterodromic $W_1W_2W_3$ in **3-II**). Similarly, the isomer **3-IV** is 3.37. 3.53 kcal/mol higher in energy than isomer **3-II** with only BSSE correction, and with BSSE and ZPE corrections. respectively. This result suggests that the spatial arrangement of the roles of hydrogen bonding (Ad, aa, A, a. etc.) in the complexes play an important role, and the switch-over of their roles would lead to substantial changes in the overall geometry and also in their stabilities.

Hydration Energies, Enthalpies and Gibbs Free Energies. In Table 3, we compare the calculated total hydration energies (ΔE_n), enthalpies (ΔH_n), and Gibbs free energies (ΔG_n) at B3LYP/6-31+G(d) level with the experimental values determined from high-pressure mass spectrometric studies[13,14] for the clustering reaction Ma + $nH_2O \rightarrow$ $Ma(H_2O)_n$ $(n = 1. 2. 3)$. The experimental values of ΔG_n at 298 K and 150 K were estimated by the equation $\Delta G_n^T = \Delta H_n^{exp} - T\Delta S_n^{exp}$ assuming ΔH_n^{exp} and ΔS_n^{exp} are temperature-independent. As illustrated in Table 3, the calculated ΔH_n and ΔG_n at 298 K and 150 K match excellently the experimental values, particularly the more recent experimental data by Meot-Ner[13] within 1 kcal/mol. These results indicate that the B3LYP/6-31+G(d) calculations used in this work are adequate in describing quantitatively the trends of the relative energetics and hydration thermodynamic functions of various isomers of $Ma(H_2O)_n$.

As mentioned previously. the hydration energy of Ma (H_2O) (-16.9 kcal/mol) is somewhat smaller than that of $NH_4^+(H_2O)$ (-19.2 kcal/mol) due to the decreased strength of charge-dipole interaction. The Gibbs free energies of the isomeric forms of $n=3$ at 298 K vary widely in the range of

Table 3. Total hydration energies (ΔE_n), enthalpies (ΔH_n), and Gibbs free energies (ΔG_n) of various isomers of $CH_3NH_3^+(H_2O)_n$ (n=1-3) for the clustering reaction $CH_3NH_3^+ + nH_2O \rightarrow CH_3NH_3^+(H_2O)_n$ at 298 K and 150 K. The values in parentheses are the relative energies with respect to the lowest energy isomers. All values are in kcal/mol

		T =298 K		T =150 K		Experimental		
	ΔE_n	ΔH_n	ΔG_n	ΔH_n	ΔG_n	ΔH_n	ΔG_n(298 K)	ΔG_n(150 K)
1	-16.86	-17.15	-9.90	-17.37	-13.59	-16.8[a], -18.8[b]	-10.3[a], -11.0[b]	-13.5[a], -14.9[b]
2-I	-30.89 (0.00)	-31.29 (0.00)	-16.64 (0.00)	-31.82 (0.00)	-24.11 (0.00)	-31.4[a], -33.4[b]	-17.7[a], -17.6[b]	-24.5[a], -25.5[b]
2-II	-28.42 (2.47)	-29.31 (1.97)	-13.59 (3.05)	-29.57 (2.26)	-21.51 (2.59)			
3-I	-42.81 (0.00)	-43.11 (0.25)	-21.73 (0.00)	-44.02 (0.00)	-32.66 (0.00)	-43.7[a], -45.8[b]	-22.8[a], -22.1[b]	-33.2[a], -33.9[b]
3-II	-41.70 (1.12)	-43.36 (0.00)	-17.32 (4.41)	-43.62 (0.40)	-30.38 (2.28)			
3-III	-41.30 (1.51)	-42.18 (1.19)	-19.66 (2.06)	-42.77 (1.24)	-31.07 (1.59)			
3-IV	-38.16 (4.65)	-39.97 (3.40)	-13.59 (8.14)	-40.17 (3.85)	-26.81 (5.85)			

[a]Reference 13. [b]Reference 14.

Table 4. Stepwise hydration energies ($\Delta E_{n-1,n}$), enthalpies ($\Delta H_{n-1,n}$) and Gibbs free energies ($\Delta G_{n-1,n}$) of various isomers of $CH_3NH_3^+(H_2O)_n$ (n=1-3) at 298 K and 150 K for the reaction $CH_3NH_3^+(H_2O)_{n-1} + H_2O \rightarrow CH_3NH_3^+(H_2O)_n$. All values are in kcal/mol

|			T =298 K		T =150 K		Experimental		
Reactant	Product	$\Delta E_{n-1,n}$	$\Delta H_{n-1,n}$	$\Delta G_{n-1,n}$	$\Delta H_{n-1,n}$	$\Delta G_{n-1,n}$	$\Delta H_{n-1,n}$	$\Delta G_{n-1,n}$ (298 K)	$\Delta G_{n-1,n}$ (150 K)
1	**2-I**	-14.03	-14.14	-6.74	-14.45	-10.52	-14.6[a], -14.6[b]	-7.4[a], -6.6[b]	-11.0[a], -10.6[b]
1	**2-II**	-11.56	-12.16	-3.69	-12.19	-7.93			
2-I	**3-I**	-11.92	-11.82	-5.09	-12.20	-8.56	-12.3[a], -12.4[b]	-5.1[a], -4.5[b]	-8.7[a], -8.4[b]
2-I	**3-II**	-10.81	-12.07	-0.68	-11.80	-6.28			
2-I	**3-III**	-10.41	-10.89	-3.02	-10.95	-6.97			
2-I	**3-IV**	-7.27	-8.68	3.05	-8.35	-2.70			
2-II	**3-II**	-13.28	-14.05	-3.72	-14.06	-8.87			
2-II	**3-III**	-12.88	-12.86	-6.07	-13.21	-9.56			
2-II	**3-IV**	-9.74	-10.65	0.01	-10.61	-5.30			

[a]Reference 13. [b]Reference 14.

-21.7 ~ -13.6 kcal/mol. and that of isomer **3-III** is 2.3 kcal/mol lower than that of isomer **3-II**. These findings are not unexpected since the entropy term involved in ΔG_n is sensitive to the temperatures as well as to the structural flexibility of each isomer. Despite the superior electronic stability of isomer **3-II** as mentioned above. the ΔG_n at 150K is 2.3, 1.6 kcal/mol higher than those of isomers **3-I** and **3-III**, respectively, suggesting that the cyclic isomer (**3-II**) is unlikely to be populated even in cold ion beam generated in a supersonic ion source. From the table. it is expected that the vibrational predissociation spectra for n=2 and n=3 are contributed predominantly from structural isomers with greater charge-dipole interactions, **2-I** and **3-I** at both temperatures.

Table 4 shows the calculated and experimental stepwise hydration energies ($\Delta E_{n-1,n}$). enthalpies ($\Delta H_{n-1,n}$), and Gibbs free energies ($\Delta G_{n-1,n}$) for the clustering reaction $Ma(H_2O)_{n-1} + H_2O \rightarrow Ma(H_2O)_n$. These results illustrate the sequential changes in the hydration energies and thermodynamic functions as one water molecule is added to the precursor complexes. For n=2. there are two types of reactions. **1** → **2-I** and **1** → **2-II**. where a charge-dipole bond and a water-water hydrogen bond are formed, respectively. The experimental $\Delta H_{n-1,n}$, $\Delta G_{n-1,n}$ match well the calculated ones for the reaction **1** → **2-I** as expected from Table 3. Another thing to notice is that the stepwise hydration energy for

1 → **2-I** (-14 kcal/mol) is smaller than that of the reaction $Ma + H_2O \rightarrow$ **1** (-16.9 kcal/mol) due to the reduced charge densities of protons. For n=3. there are seven types of reactions. four from precursor isomer **2-I** and three from **2-II**. The stepwise hydration energies vary widely from 7.27 kcal/mol to 11.92 kcal/mol depending on the binding sites of precursor isomers for the third water molecule. The **2-I** → **3-I** reaction forming a charge-dipole bond has the greatest stepwise hydration energy while the **2-I** → **3-IV** reaction forming an asymmetric ring network has the smallest value. Moreover. the positive $\Delta G_{n-1,n}$ for the latter reaction at 298 K suggests that this reaction is unlikely to occur at 298 K. The experimental values of $\Delta H_{n-1,n}$, $\Delta G_{n-1,n}$ match well the calculated ones for the **2-I** → **3-I** reaction.

Vibrational Spectra. Figure 2 depicts the *ab initio* predicted stick spectra for various isomers of $Ma(H_2O)_n$ (n=1-3) in the 2600-3800 cm^{-1} region together with that of free Ma. The scaled frequencies, the IR intensities. and the assignments are listed in Table 5. For free Ma. the symmetric and antisymmetric NH_3 stretches at 3306 and 3387 cm^{-1} are two intense features in the spectrum while the C-H stretches are very weak in intensity. For n=1. the bonded-NH(1) stretch (2962 cm^{-1}) is greatly red-shifted from that of free Ma due to the combined effects of the N-H bond weakening by charge-dipole interaction and the slight increases in the reduced
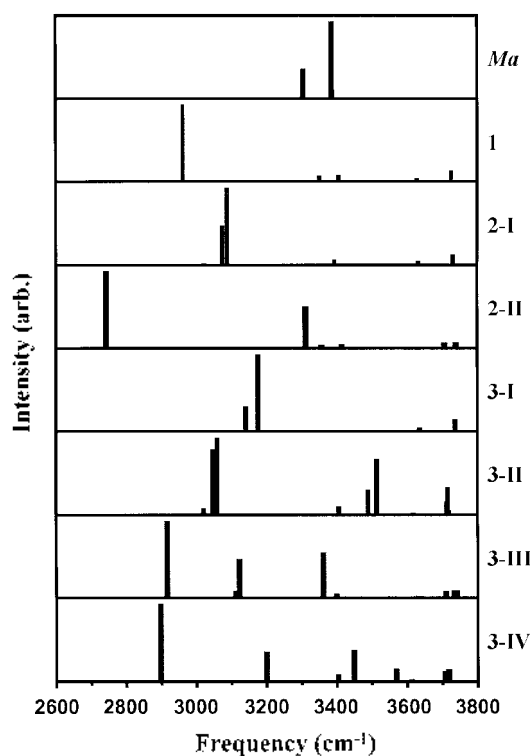
Figure 2. *Ab initio* predicted stick spectra of various isomers of $CH_3NH_3^+(H_2O)_n$ $(n=0\text{-}3)$ at B3LYP/6-31+G(d) level.

Table 5. *Ab initio* scaled frequencies (cm^{-1}), IR absorption intensities (km/mol), and assignments for C-H, N-H, and O-H stretches of $CH_3NH_3^+(H_2O)_n$ $(n=1\text{-}3)$

	Frequency	Intensity	Assignments[a]
1	3725.6	154.3	Antisymmetric free-OH(1)
	3628.8	50.3	Symmetric free-OH(1)
	3406.7	87.9	Antisymmetric free-NH
	3352.2	78.0	Antisymmetric free-NH
	3123.9	0.0	Antisymmetric CH₃
	3122.9	0.2	Antisymmetric CH₃
	3026.8	5.6	Symmetric CH₃
	2962.0	1042.6	Bonded-NH(1)
2-I	3731.5	131.3	Antisymmetric free-OH(1)
	3731.2	146.1	Antisymmetric free-OH(2)
	3632.6	26.8	Symmetric (symmetric free-OH(1) and symmetric free-OH(2))
	3632.3	55.7	Antisymmetric (symmetric free-OH(1) and symmetric free-OH(2))
	3394.8	76.9	free-NH
	3117.8	7.9	Antisymmetric CH₃
	3115.9	15.2	Antisymmetric CH₃
	3088.6	1059.2	Antisymmetric bonded-NH(1,2)
	3074.7	543.3	Symmetric bonded-NH(1,2)
	3021.9	24.6	Symmetric CH₃
2-II	3739.3	128.1	Antisymmetric free-OH(2)
	3706.5	122.8	free-OH(1)
	3636.2	31.0	Symmetric free-OH(2)
	3415.0	80.4	Antisymmetric free-NH
	3357.3	69.6	Symmetric free-NH
	3312.4	912.9	Bonded-OH(1)
	3120.8	0.1	Antisymmetric CH₃
	3118.3	0.1	Antisymmetric CH₃

Table 5. Continued

	Frequency	Intensity	Assignments[a]
	3024.6	1.1	Symmetric CH₃
	2743.1	1683.3	Bonded-NH(1)
3-I	3736.1	124.9	Antisymmetric free-OH(1)
	3736.0	122.6	Antisymmetric free-OH(2)
	3735.8	132.7	Antisymmetric free-OH(3)
	3635.1	15.2	Symmetric (symmetric free-OH(1) and symmetric free-OH(2) and symmetric free-OH(3))
	3634.9	45.6	Antisymmetric (symmetric free-OH(1) and symmetric free-OH(2) and symmetric free-OH(3))
	3634.5	43.0	Antisymmetric (symmetric free-OH(1) and symmetric free-OH(2) and symmetric free-OH(3))
	3176.3	846.5	Antisymmetric bonded-NH(1,2,3)
	3176.0	845.3	Antisymmetric bonded-NH(1,2,3)
	3140.9	268.9	Symmetric bonded-NH(1,2,3)
	3109.7	14.1	Antisymmetric CH₃
	3109.5	14.0	Antisymmetric CH₃
	3019.1	13.2	Symmetric CH₃
3-II	3717.3	42.1	Symmetric free-OH(1,2)
	3714.0	282.8	Antisymmetric free-OH(1,2)
	3711.8	135.0	Antisymmetric free-OH(3)
	3615.6	17.1	Symmetric free-OH(3)
	3512.6	570.9	Symmetric bonded-OH(1,2)
	3488.7	258.5	Antisymmetric bonded-OH(1,2)
	3405.2	89.6	free-NH
	3116.2	0.3	Antisymmetric CH₃
	3112.2	0.7	Antisymmetric CH₃
	3058.2	791.5	Symmetric bonded-NH(1,2)
	3045.9	669.9	Antisymmetric bonded-NH(1,2)
	3019.9	70.2	Symmetric CH₃
3-III	3741.6	123.0	Antisymmetric free-OH(3)
	3734.4	131.0	Antisymmetric free-OH(2)
	3710.1	116.6	free-OH(1)
	3637.2	26.4	Symmetric free-OH(3)
	3633.9	29.0	Symmetric free-OH(2)
	3399.9	73.3	free-NH
	3361.3	761.7	Bonded-OH(1)
	3122.6	651.4	Bonded-NH(2) and antisymmetric CH₃
	3115.4	11.6	and antisymmetric CH₃
	3112.0	118.3	Bonded-NH(2) and antisymmetric CH₃
	3022.4	15.1	Symmetric CH₃
	2915.8	1285.5	Bonded-NH(1)
3-IV	3718.8	156.0	free-OH(2)
	3716.2	162.2	Antisymmetric (free-OH(3) and bonded-OH(3))
	3707.3	132.5	Antisymmetric free-OH(1)
	3612.2	27.1	Symmetric free-OH(1)
	3568.8	168.5	Symmetric (free-OH(3) and bonded-OH(3))
	3448.8	411.3	Bonded-OH(2)
	3403.7	94.9	free-NH
	3199.8	391.3	Bonded-NH(1)
	3118.8	0.3	Antisymmetric CH₃
	3111.9	2.4	Antisymmetric CH₃
	3021.2	3.5	Symmetric CH₃
	2897.4	1022.1	Bonded-NH(2)

[a]Numbers in parentheses denote numbers of H_2O molecules in the complexes according to Figure 1.

mass of N-H. The oscillator strength of bonded-NH stretch is predicted to be much greater than those of remaining free NH stretches. The symmetric and antisymmetric free OH stretches of A-type $1^\circ H_2O$ (3629, 3726 cm^{-1}) are slightly red-shifted from those of free H_2O (3636, 3756 cm^{-1}).

In isomer **2-I**, the symmetric and antisymmetric bonded-NH(1,2) stretches appear at 3075, 3089 cm^{-1}. less red-shifted from free Ma than isomer **1** which is consistent with the decreased strengths of individual charge-dipole interactions for **2-I**. The symmetric and antisymmetric free OH stretches of two A-type $1^\circ H_2O(1,2)$ molecules are resonated at similar frequencies as in isomer **1**. In isomer **2-II**, the bonded-NH stretch (2743 cm^{-1}) with greater oscillator strength is more red-shifted from that of isomer **1** due to the increased strength of localized charge-dipole interaction as mentioned previously. The bonded-OH stretch of an Ad-type $1^\circ H_2O(1)$ (3312 cm^{-1}) is greatly red-shifted from the OH stretches of free H_2O. and the free OH stretch of the $1^\circ H_2O(1)$ (3706 cm^{-1}) appears in-between the symmetric and antisymmetric free OH stretches of a-type $2^\circ H_2O(2)$ (3636, 3739 cm^{-1}). Since there are remarkable differences in the spectral patterns between two isomers, their contributions to the vibrational predissociation spectrum can be easily resolved, although isomer **2-I** has much higher population in ion beam.

For isomer **3-I**, the symmetric and antisymmetric bonded-NH₃ stretches (3141, 3176 cm^{-1}) are less red-shifted from those of free Ma than those of isomers **1** and **2-I**, which leads to the finding that the average red-shifts of bonded-NH stretches for isomers **1**, **2-I**, **3-I** (398, 278, 196 cm^{-1}) from that of free Ma decrease gradually as the strengths of individual charge-dipole interactions decrease. The symmetric and antisymmetric free OH stretches of three A-type $1^\circ H_2O(1,2,3)$ molecules appear at 3635, 3736 cm^{-1}. In isomer **3-II**, the symmetric and antisymmetric bonded-NH stretches (3058, 3046 cm^{-1}) are ~308 cm^{-1} red-shifted on average from that of free Ma, which is greater than that of isomer **2-I** (278 cm^{-1}) despite the weaker direct charge-dipole interactions for the former due to the ring strains. This result suggest that the indirect charge-dipole interactions between two protons H(1,2) and $2^\circ H_2O(3)$ and the attractive three-body interactions (MaW₁W₃, MaW₁W₃) may be responsible for the weakened NH(1,2) bonds of isomer **3-II**.

The symmetric and antisymmetric bonded-OH stretches of two Ad-type $1^\circ H_2O(1,2)$ molecules that are considered as a signature of cyclic ion-(water)₃ isomer[12,16] appear at 3512, 3489 cm^{-1}, ~196 cm^{-1} red-shifted on average from that of free water molecule. The symmetric and antisymmetric free OH stretches of two Ad-type $1^\circ H_2O(1,2)$ (3717, 3714 cm^{-1}) are somewhat blue-shifted from those of similar Ad-type $1^\circ H_2O$ molecule of isomer **2-II** (3706 cm^{-1}). The symmetric and antisymmetric free OH stretches of one aa-type $2^\circ H_2O(3)$ molecule (3616, 3711 cm^{-1}) are somewhat red-shifted from those of A-type $1^\circ H_2O$ (~3630, ~3735 cm^{-1}) in isomers **1**, **2-I**, **3-I**, and those of a-type H_2O (~3635, ~3740 cm^{-1}) in isomers **2-II**, **3-III**. These results suggest that the distinct free OH stretch frequencies depending on the hydro-

gen bond roles of water molecules despite of the small differences could also play as a structural fingerprint.

In isomer **3-III**, there are two types of bonded-NH stretches one water-bonded-NH(2) stretch mixed with antisymmetric CH₃ stretch, and two water-bonded NH(1). The former mixed modes (3112, 3123 cm^{-1}) are ~243 cm^{-1} red-shifted from that of free Ma while the latter (2916 cm^{-1}) is 444 cm^{-1} red-shifted. The larger red-shift of bonded-NH(1) stretch than that of isomer **1** is attributed to the localized indirect charge-dipole interaction of $2^\circ H_2O(3)$ and three-body attractive interaction (MaW₁W₃) toward the NH(1) bond. The bonded-OH stretch of Ad-type $1^\circ H_2O(1)$ is resonated at 3361 cm^{-1}, somewhat blue-shifted from that of isomer **2-II** (3312 cm^{-1}).

As depicted in Figure 2. the spectral pattern of cyclic isomer **3-IV** is closer in appearance to that of isomer **3-III** than another cyclic isomer **3-II**. This finding is not unexpected since the hydrogen bond between $H_2O(1)$ and $H_2O(3)$ in isomer **3-IV** is substantially lengthened (2.06 Å) compared to the hydrogen bond between $H_2O(2)$ and $H_2O(3)$ (1.86 Å) resulting in less vibrational coupling between the $H_2O(1)$ and $H_2O(2,3)$ moieties. The bonded-NH(1) and NH(2) stretches appear separately at 3200, 2897 cm^{-1} reflecting the distinct nature of two charge-dipole bonds consistent with the different hydrogen bond lengths (R(H$_K^1$O₁)=1.95 Å, R(H$_K^2$O₂)=1.69 Å). The ~20 cm^{-1} red-shift of the bonded-NH(2) stretch from bonded-NH(1) stretch of isomer **3-III** is attributed to the more localized charge densities in proton (H$_K^2$) arising from the weakened charge-dipole interaction between proton (H$_K^1$) and $1^\circ H_2O(1)$ due to the longer distance. The bonded-OH stretch of Ad-type $1^\circ H_2O(2)$ appear at 3449 cm^{-1}, 90 cm^{-1} blue-shifted from that of Ad-type $1^\circ H_2O(1)$ in isomer **3-III** consistent with the weaker $H_2O(2)$-$H_2O(3)$ hydrogen bonding due to the substantially bent hydrogen bond angle ($\angle O_2H_2^3O_3 =145.3^\circ$). Conversely, the bonded and free OH stretches of ad-type $2^\circ H_2O(3)$ are mixed to form the symmetric and antisymmetric mixed OH stretches at 3612, 3716 cm^{-1} due to the extremely weak hydrogen bond interaction between $H_2O(1)$ and $H_2O(3)$ in isomer **3-IV**. The symmetric and antisymmetric free OH stretches of Aa-type $1^\circ H_2O(1)$ are resonated at 3612, 3707 cm^{-1}, somewhat different from other types of free OH stretches (A, a, Ad, ad, aa) mentioned above.

In summary, the vibrational patterns for various structural isomers of Ma(H₂O)ₙ (n=1-3) depend on the overall structures as well as the local hydrogen bond interactions. The bonded-NH stretches range from 2743 cm^{-1} to 3200 cm^{-1} depending on the isomeric structures, and also the average red-shifts from that of free Ma (3360 cm^{-1}) correlate excellently with the strengths of local many-body interactions between Ma core and surrounding water molecules. The distinct bonded-OH stretch frequencies (3300-3500 cm^{-1}) depending on the shapes of structures and the roles of ligands (Ad, ad) play a role as fingerprint for the water-water hydrogen bond interactions. For instance, the doublet spectral pattern near 3500 cm^{-1} is considered as signature of cyclic ion-(water)₃ structure with two Ad-type H_2O mole-

cules. The free OH stretches are relatively insensitive to the local hydrogen bond interactions, but the recognizable differences in the frequencies depending on the roles of ligands such as ~3730, ~3630 cm^{-1} for A-type $1^\circ H_2O$, ~3740, ~3636 cm^{-1} for a-type $2^\circ H_2O$, 3707, 3612 cm^{-1} for Aa-type $1^\circ H_2O$. 3712, 3616 cm^{-1} for aa-type $2^\circ H_2O$, and 3710~3720 cm^{-1} for Ad-type $1^\circ H_2O$ can be used for further spectral evidences in identifying the structural isomers of protonated ion-water complexes.

Conclusions

In this work the B3LYP/6-31+G(d) method has been applied to investigate the structural isomers, the hydration energies, the thermodynamic functions, and the vibrational spectra of various isomers of $CH_3NH_3^-(H_2O)_n$ (n=1,2,3) in comparison with the available experimental thermochemical data. Results indicate that not only the direct charge-dipole two-body interactions, but also the three-body interactions involving water-water hydrogen bonding and indirect charge-dipole interactions play significant roles in determining the overall structures and relative stabilities of isomers. Particularly, the hydrogen bond cooperativity plays a critical role in stabilizing the cyclic isomer *vs.* tripod isomer for n=3. The calculated thermodynamic functions match well the recent experimental thermodynamic functions by Meot-Ner within 1 kcal/mol. The trends of calculated hydration energies and the vibrational frequencies of bonded-NH, bonded-OH, and free OH stretches correlate excellently with the differences in their local many-body hydrogen bond interactions in each isomer. It is proposed that the distinct spectral patterns of individual isomers can be used as fingerprints in identifying the structural isomers that contribute to the vibrational predissociation spectra.

References

1. Tarek, M.; Tobias, D. J. *J. Am. Chem. Soc.* **1999**, *121*, 9740. Cleland, W. W.; Kreevoy, M. M. *Science* **1994**, *264*, 1887. Creighton, T. E. *Proteins: Structure and Molecular Properties*; Freeman: New York, 1993.
2. Woenckhaus, J.; Hudgins, R. R.; Jarrold, M. F. *J. Am. Chem. Soc.* **1997**, *119*, 9586. Marx, D. M.; Tuckerman, M. E.; Hutter, J.; Parrinello, M. *Nature* **1999**, *397*, 601.
3. Mao, Y.; Ratner, M. A.; Jarrold, M. F. *J. Am. Chem. Soc.* **2000**, *122*, 2950. Hill, R. B.; Hong, J.; DeGrado, W. F. *J. Am. Chem. Soc.* **2000**, *122*, 746.
4. Jarrold, M. *Acc. Chem. Res.* **1999**, *32*, 360. Clary, D. C.; Benoit, D. M.; Mourik, T. V. *Acc. Chem. Res.* **2000**, *33*, 441.
5. Chang, H. C.; Jiang, J. C.; Hahndorf, I.; Lin, S. H.; Lee, Y. T.; Chang, H. C. *J. Am. Chem. Soc.* **1999**, *121*, 4443.
6. Wu, C. C.; Jiang, J. C.; Boo, D. W.; Lin, S. H.; Lee, Y. T.; Chang, H. C. *J. Chem. Phys.* **2000**, *112*, 176.
7. Chang, H. C.; Jiang, J. C.; Lin, S. H.; Lee, Y. T.; Chang, H. C. *J. Phys. Chem. A* **1999**, *103*, 2941.
8. Jiang, J. C.; Wang, Y. S.; Chang, H. C.; Lin, S. H.; Lee, Y. T.; Niedner-Schattenburg, G.; Chang, H. C. *J. Am. Chem. Soc.* **2000**, *122*, 1398.
9. Bieske, E. J.; Maier, J. P. *Chem. Rev.* **1993**, *93*, 2603.
10. Bandyopadhyay, P.; Gordon, M. S. *J. Chem. Phys.* **2000**, *113*, 1104.
11. Tomasi, J.; Perisco, M. *Chem Rev.* **1994**, *94*, 2027.
12. Boo, D. W *Bull. Korean Chem. Soc.* (submitted). Boo, D. W.; Chang, H. C.; Lee, Y. T. *J. Phys. Chem. A* (submitted).
13. Meot-Ner, M. *J. Am. Chem. Soc.* **1984**, *106*, 1265.
14. Lau, Y. K.; Kebarle, P. *Can. J. Chem.* **1981**, *59*, 151.
15. Jiang, J. C.; Chang, H. C.; Lee, Y. T.; Lin, S. H. *J. Phys. Chem. A* **1999**, *103*, 3123.
16. Wang, Y. S.; Chang, H. C.; Jiang, J. C.; Lin, S. H.; Lee, Y. T.; Chang, H. C. *J. Am. Chem. Soc.* **1998**, *120*, 8777.
17. Frisch, M. J. *et al. GAUSSIAN 98*; Gaussian, Inc.: Pittsburgh, Pennsylvania, 1998.
18. Boys, S. F.; Bernardi, F. *Mol. Phys.* **1970**, *19*, 553.
19. Lee, S. W.; Cox, H.; Goddard, W. A. III; Beauchamp, J. L. *J. Am. Chem. Soc.* **2000**, *122*, 9201.
20. Xantheas, S. S. *J. Chem. Phys.* **1994**, *100*, 7523.